MOLECULAR AND CELLULAR BIOLOGY, June 2001, p. 3642–3651 Vol. 21, No. 11
0270-7306/01/$04.00+0 DOI: 10.1128/MCB.21.11.3642–3651.2001

The Absence of the DNA-Dependent Protein Kinase Catalytic Subunit in Mice Results in Anaphase Bridges and in Increased Telomeric Fusions with Normal Telomere Length and G-Strand Overhang

FERMÍN A. GOYTISOLO,[1] ENRIQUE SAMPER,[1] SCOTT EDMONSON,[2] GUILLERMO E. TACCIOLI,[2] AND MARÍA A. BLASCO[1]*

Department of Immunology and Oncology, Centro Nacional de Biotecnología, Madrid E-28049, Spain,[1] and Department of Microbiology, Boston University School of Medicine, Boston, Massachusetts 02118-2526[2]

Received 2 November 2000/Returned for modification 11 December 2000/Accepted 23 February 2001

The major pathway in mammalian cells for repairing DNA double-strand breaks (DSB) is via nonhomologous end joining. Five components function in this pathway, of which three (Ku70, Ku80, and the DNA-dependent protein kinase catalytic subunit [DNA-PKcs]) constitute a complex termed DNA-dependent protein kinase (DNA-PK). Mammalian Ku proteins bind to DSB and recruit DNA-PKcs to the break. Interestingly, besides their role in DSB repair, Ku proteins bind to chromosome ends, or telomeres, protecting them from end-to-end fusions. Here we show that DNA-PKcs$^{-/-}$ cells display an increased frequency of spontaneous telomeric fusions and anaphase bridges. However, DNA-PKcs deficiency does not result in significant changes in telomere length or in deregulation of the G-strand overhang at the telomeres. Although less severe, this phenotype is reminiscent of the one recently described for Ku86-defective cells. Here we show that, besides DNA repair, a role for DNA-PKcs is to protect telomeres, which in turn are essential for chromosomal stability.

One of the most lethal lesions that can occur in a cell after ionizing irradiation is a double-strand break (DSB), because it disrupts the integrity of the DNA molecule. The importance of this lesion is evident by the existence of evolutionarily conserved DNA repair systems that act on DSBs. Moreover, DSBs are also generated under physiological conditions, such as during transposition, meiosis, and recombination. It is important that these endogenous breaks be resolved in order for cells to function properly. Cells have evolved two fundamentally different pathways for repairing DSBs: homologous recombination (HR), which requires extensive regions of homology, and DNA nonhomologous end joining (NHEJ). In contrast to what has been described for *Saccharomyces cerevisiae*, the major pathway in mammalian cells is NHEJ. Five components function in this pathway, of which three (Ku70, Ku80, and the DNA-dependent protein kinase catalytic subunit [DNA-PKcs]) constitute a complex termed DNA-dependent protein kinase (DNA-PK) (48). Xrcc4 and DNA ligase IV are the two additional proteins known to function in the NHEJ pathway (19, 22, 37). The essential role of the DNA-PK complex in NHEJ has been well documented in mice generated by HR and carrying null mutations for any of the three subunits. The phenotypes shared by these animals are defective DSB repair (dsbr), and thus hypersensitivity to ionizing radiation, and an impaired V(D)J recombination process (18, 25, 43, 44, 49, 52). However, these animals present differential phenotypes, which provides unequivocal evidence for additional roles for each component of the DNA-PK complex separate from their function in NHEJ. In this context, Ku-deficient mice grow poorly and senesce early (25, 36, 43, 51), a differential feature not observed in DNA-PKcs-deficient mice (18, 49).

Telomeres are unique structures present at the end of eukaryotic chromosomes and are composed of tandem DNA repeats and specific proteins, conferring properties that keep the ends from being detected as DSBs by the cell (7). The fundamental difference between telomeres and DSBs is that telomeres are protected from end-to-end fusions, recombination, and unregulated nucleolytic degradation, whereas DSBs are subjected to such processing events in order to promote repair of the break. In fact, when normal telomere function is affected, either by loss of telomeric sequences or by mutation of a protective telomere binding protein, i.e., TRF2, end-to-end fusions occur (9, 14, 50). Telomeric sequences are lost during in vitro culture of primary cells and with increasing age in some adult tissues. Besides, an impairment of telomere function due to a loss of telomeric sequences has been shown to limit the proliferative capacity of cultured cells and to affect the life span of the organism (4, 10).

Studies of yeast, where the major DNA repair pathway is HR instead of NHEJ, show that Ku has an important role at the telomere. In particular, yeast defective in either Ku subunit show a 60% loss of telomeric repeats, loss of telomere clustering, loss of telomeric silencing, and deregulation of the G-strand overhang (12, 13, 21, 35, 42). Furthermore, yeast Ku moves from the telomeres to the DSB upon induction of damage, suggesting a link between DNA repair and telomeres (38, 40). In mammals, Ku proteins have been reported to bind to telomeric sequences (6, 31) and to prevent end-to-end fusions (5, 32, 47); but in contrast to what has been reported for yeast, Ku86 deficiency in mice does not result in telomere shortening or in deregulation of the G-strand overhang (47). It is likely

* Corresponding author. Mailing address: Department of Immunology and Oncology, Centro Nacional de Biotecnología, Madrid E-28049, Spain. Phone: 34-915854846. Fax: 34-913720493. E-mail: mblasco@cnb.uam.es.

TABLE 1. Q-FISH and cytogenetic analysis of wild-type and DNA-PKcs$^{-/-}$ MEFs

Litter	Genotype	Chr.[a] arm	Telomere length (kb) (SD, SE)	No. of chr. aberrations			No. of metaphases
				Telomere fusions[b]	Chr. breaks or fragments[c]	Telomere associations[d]	
A1	−/−	p	28.24 (9.78, 0.2)	6	4	7	100
		q	33.66 (11.38, 0.23				
		Avg	30.95 (10.58, 0.219)				
A2	+/−	p	29.5 (9.41, 0.19)	6	2	14	100
		q	34.92 (10.6, 0.021)				
		Avg	32.21 (10.01, 0.2)				
B6	−/−	p	31.65 (10.73, 0.219)	7	2	21	100
		q	36.5 (10.24, 0.209)				
		Avg	34.08 (10.48, 0.21)				
B5	WT[e]	p	32.61 (11.17, 0.22)	2	2	13	100
		q	37.7 (10.03, 0.2)				
		Avg	35.15 (10.6, 0.21)				
C2	−/−	p	34.56 (9.49, 0.19)	6	4	19	100
		q	40.27 (11.13, 0.22)				
		Avg	37.42 (10.31, 0.21)				
C5	WT	p	30.81 (8.61, 0.17)	1	4	10	80
		q	38.97 (9.94, 0.2)				
		Avg	34.89 (9.28, 0.19)				
C3	WT	p	31.58 (10.54, 0.21)	2	3	10	100
		q	38.45 (11.8, 0.24)				
		Avg	35.01 (11.17, 0.22)				
C9	−/−	p	27.78 (8.22, 0.16)	6	0	11	80
		q	32.92 (9.96, 0.2)				
		Avg	30.35 (9.09, 0.18)				

[a] Chr., chromosome.
[b] Average numbers per metaphase: wild type, 0.017; DNA-PKcs$^{-/-}$, 0.065.
[c] Average numbers per metaphase: wild type, 0.032; DNA-PKcs$^{-/-}$, 0.026.
[d] Average numbers per metaphase: wild type, 0.012; DNA-PKcs$^{-/-}$, 0.015.
[e] WT, wild type.

that Ku protects mammalian telomeres from fusions through its interaction with another telomeric protein, TRF1 (32). DNA-PKcs is a member of the phosphatidylinositol 3-kinase superfamily (27, 45), which includes, among others, the yeast Tel1 protein and human ATM, which have been implicated in telomere metabolism (23, 39, 41). Preliminary evidence suggesting a role for DNA-PKcs at the telomeres came from studies conducted with severe combined immunodeficient (SCID) mice carrying a leaky mutation in the DNA-PKcs locus. These studies showed that SCID mouse telomeres were elongated compared to those of wild-type mice and that SCID mouse cells had an increased frequency of end-to-end fusions (2, 5,11, 15, 26, 33). In addition, the Mre11-Rad50-NsbI dsbr complex is also present at the mammalian telomere and interacts with telomeric protein TRF2 (53). Collectively, the recruitment of DSB DNA repair proteins to the telomeres suggests that chromosome ends are binding sites for dsbr proteins in mammals.

In the present study, the use of mice with a null mutation in the DNA-PKcs gene (49) allowed us to demonstrate that the absence of DNA-PKcs in mammals results in an increased frequency of telomeric fusions and anaphase bridges, suggesting a protective role of DNA-PKcs at the telomere independent to that reported for Ku proteins (32, 47). Interestingly, DNA-PKcs deficiency, similar to Ku86 deficiency, does not result in an alteration of telomere length or the integrity of the G-strand overhang. In this context, the contrasting results found for SCID mice that show elongated telomeres compared to those of wild-type controls (26) (see below) might serve as a means to discover important differences between these two mouse models.

MATERIALS AND METHODS

Mice and cells. DNA-PKcs null mice were described elsewhere (49). Wild-type and DNA-PKcs$^{-/-}$ mice or cells were derived from heterozygous crosses and, for all work, littermate mice or cells were used. SCID mice used were BALB/cJHanHsd-Scid (Harlam, Barcelona, Spain), and the corresponding wild-type mice in the same genetic background were BALB/cOlaHsd (Harlam). Mice used for quantitative fluorescent in situ hybridization (Q-FISH) and flow cytometry FISH (Flow-FISH) studies were between 8 and 12 weeks old. Mouse embryonic fibroblasts (MEFs) were prepared from day 13.5 embryos derived from heterozygous crosses as described previously (9). First-passage MEFs used in the different experiments corresponded to approximately two population doublings (PDL 2). Mice or cells from the same litter are indicated with the same letter.

Scoring of chromosomal abnormalities. Between 80 and 100 (each) wild-type, DNA-PKcs$^{+/-}$, and DNA-PKcs$^{-/-}$ metaphases were scored for telomere fusions, chromatid breaks, and chromosome fragments by superimposing the telomere image on the DAPI (4′,6′-diamidino-2-phenylindole) chromosome image in the TFL-telo program. The following criteria were applied: telomeric fusions, chromosomes fused by their telomeres showing at least two overlapping telomeric signals; Robertson-like fusions, chromosomes fused by their p arms (they may or may not show telomeres at the fusion point; all the Robertson-like fusions found in this study showed telomeres at the fusion point and were included in the group of telomeric fusions); telomere associations, chromosomes with four distinct telomere signals but aligned less than one-half chromatid apart; breaks, gaps in a chromatid whose corresponding chromosome was identified; chromosome fragments, chromosome pieces (with two telomeres or less) whose corresponding chromosome was not easily identified.

To score for anaphase bridges, primary MEF cultures were seeded on microscope slides and stained with DAPI to visualize the DNA. At least 50 anaphases were scored for wild-type and DNA-PKcs$^{-/-}$ cultures, and the anaphase bridges were counted.

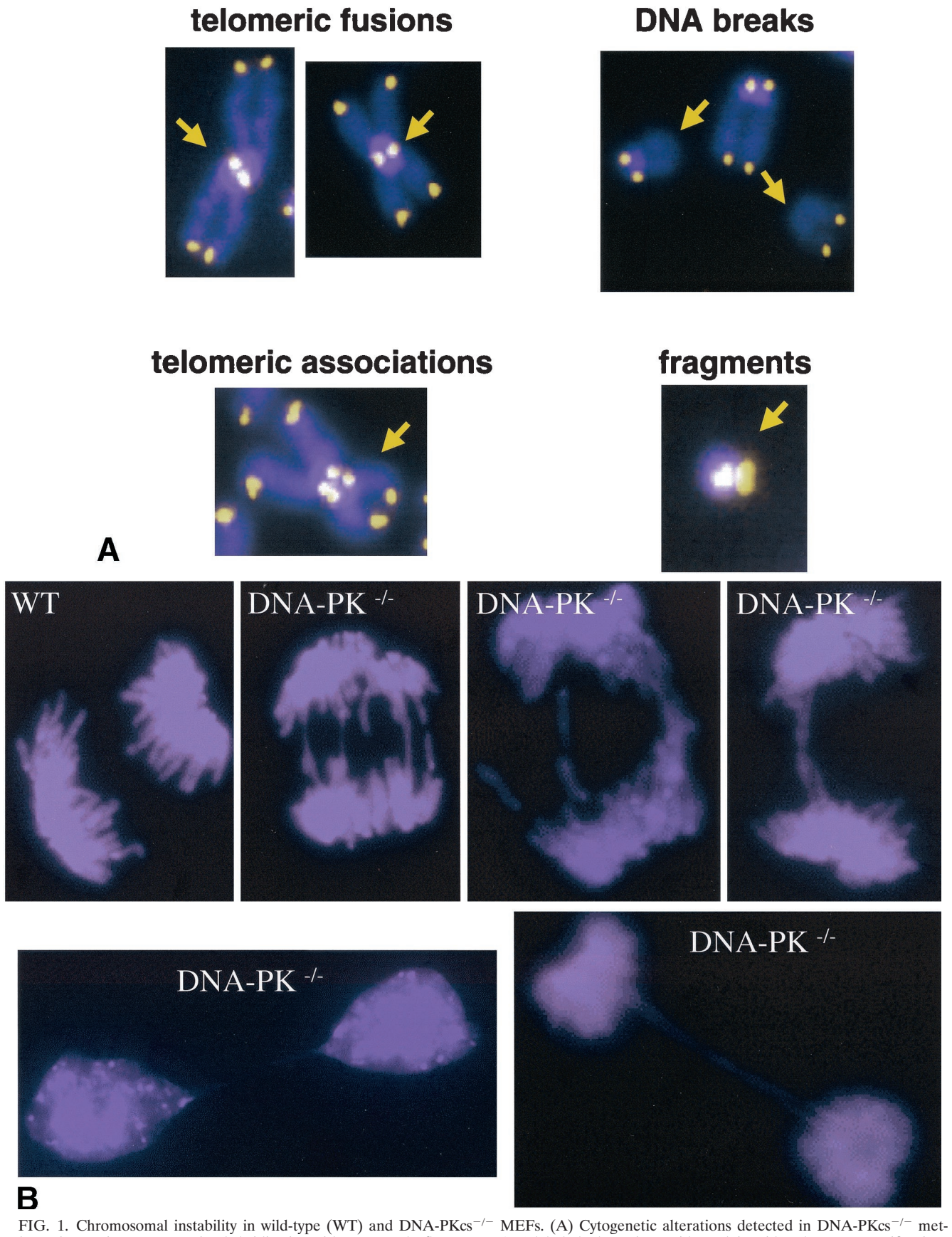

FIG. 1. Chromosomal instability in wild-type (WT) and DNA-PKcs$^{-/-}$ MEFs. (A) Cytogenetic alterations detected in DNA-PKcs$^{-/-}$ metaphases from primary MEFs after hybridization with DAPI and a fluorescent Cy-3-labeled telomeric peptide nucleic acid probe. For quantifications see Table 1. Blue, chromosome DNA stained with DAPI; yellow and white dots, TTAGGG repeats; yellow arrows, chromosomal abnormalities. For definition of the different aberrations see Materials and Methods. (B) Representative images of anaphase bridges in DNA-PKcs$^{-/-}$ cells. Blue, chromosome DNA stained with DAPI. Notice the presence of DNA bridges in DNA-PKcs-deficient cells even in late-anaphase and telophase stages.

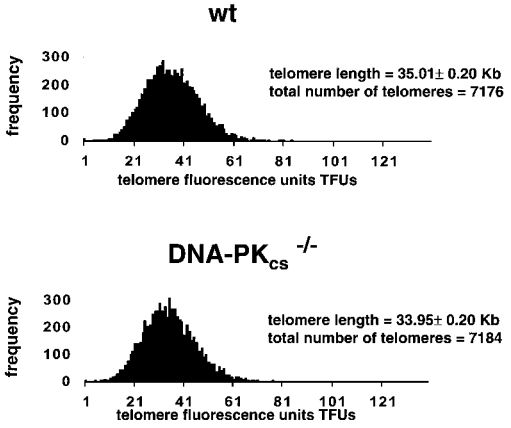

FIG. 2. Telomere fluorescence distribution in wild-type (wt), DNA-PKcs$^{+/-}$, and DNA-PKcs$^{-/-}$ MEFs. Shown is the telomere length distribution of at least 7,100 telomeres in primary MEFs from three different littermate wt (B5, C5, and C3) and DNA-PKcs$^{-/-}$ (B6, C2, and C9) mice. The histograms depict similar telomeres in DNA-PKcs$^{-/-}$ and wt cells. One telomere fluorescence unit corresponds to 1 kb of TTAGGG repeats (see Tables 1 and 2 for telomere length values).

Statistical analysis. Statistical calculation was done using Microsoft Excel. For statistical significance, Student's *t* test values were calculated.

Telomere length analysis. (i) Q-FISH. First-passage MEFs were prepared for Q-FISH as described previously (29). Q-FISH was carried out as described previously (29, 34, 47). To correct for lamp intensity and alignment, images from fluorescent beads (Molecular Probes) were analyzed using the TFL-Telo program. Telomere fluorescence values were extrapolated from the telomere fluorescence of LY-R and LY-S lymphoma cell lines (1) of known lengths of 80 and 10 kb (E. Samper et al., unpublished results). There was a linear correlation (r^2 = 0.999) between the fluorescence intensities of the LY-R and -S telomeres with a slope of 38.6. The calibration-corrected telomere fluorescence intensity was calculated as described previously (29).

Images were recorded using a COHU charge-coupled device camera on a Leica Leitz DMRB fluorescence microscope. A Philips CS 100W-2 mercury vapor lamp was used as the source. Images were captured using Leica Q-FISH software at a 400-ms integration time in a linear-acquisition mode to prevent oversaturation of fluorescence intensity.

TFL-Telo software (gift from P. M. Lansdorp, Vancouver, British Columbia, Canada) was used to quantify the fluorescence intensity of telomeres from at least 15 metaphases or fusions of each data point. The images from littermate wild-type and DNA-PKcs$^{-/-}$ metaphases were captured on the same day, in parallel, and blindly. All the images from the MEFs were captured in a 3-day period after the hybridization.

TABLE 2. Measurement by Flow-FISH of telomere length in MEFs obtained from DNA-PKcs$^{+/-}$ heterozygous crosses

Embryo	Litter	Genotype	Telomere length[a]
A1	1	−/−	2.45
A2		+/−	2.91
B3	2	+/−	2.53
B4		−/−	2.58
B5		+/+	2.56
B6		−/−	2.68
C2	3	−/−	2.68
C3		+/+	2.76
C5		+/+	2.82
C9		−/−	2.51

[a] Telomere length is expressed in arbitrary fluorescence units which have been normalized against a calibration curve on R and S cells (see Materials and Methods).

TABLE 3. Measurement by Flow-FISH of telomere length in splenocytes and BM cells obtained from DNA-PKcs$^{+/+}$, DNA-PKcs$^{+/-}$, and DNA-PKcs$^{-/-}$ mice

Mouse (sex[c])	Litter	Genotype	Telomere length[a] for:	
			Splenocytes	BM cells
D33 (F)	1	−/−	3.55	
D34 (F)		+/+	2.83	
D36 (M)	2	−/−	3.20	
D44 (F)		+/−	2.82	
D49 (F)	3	−/−	3.08	
D54 (F)		+/−	2.29	
DA38 (F)	4	−/−	3.49	3.56
DA39 (F)		−/−	3.43	3.33
DA40 (F)		+/+	3.34	3.29
DA45 (M)	5	+/+	3.69	3.08
DA46 (M)		+/+	3.56	3.47
DA47 (F)		−/−	3.73	4.01
DA48 (F)		−/−	3.93	3.29
DA50 (M)	6	+/−	3.77	3.14
DA51 (M)		+/−	4.07	3.41
DA52 (M)		−/−	4.11	3.48
DA58 (M)	7[b]	−/−	3.15	3.59
DA59 (M)		+/−	3.65	3.05
DA60 (M)		+/+	3.75	3.74
DA61 (F)		−/−	3.82	3.51
DA62 (F)		−/−	3.98	3.44
DA64 (F)		+/+	4.22	3.55

[a] Telomere length is expressed in arbitrary fluorescence units which have been normalized against a calibration curve on R and S cells (see Materials and Methods).
[b] The animals of litter 7 were analyzed in two different experiments.
[c] M, male; F, female.

(ii) Flow-FISH. Fresh bone marrow (BM) cells, splenocytes, and primary MEFs from littermate wild-type, DNA-PKcs$^{+/-}$, and DNA-PKcs$^{-/-}$ mice, as well as splenocytes and BM cells from SCID and control wild-type animals, were prepared as described previously (9, 29, 30). Flow-FISH was performed as described previously(46). To normalize Flow-FISH data two mouse leukemia cell lines (LY-R and LY-S; described above) were used as internal controls in each experiment. The telomere fluorescence of at least 2,000 cells gated at the G_1-G_0 cell cycle stage was measured using a Coulter flow EPICS XL cytometer with SYSTEM 2 software.

(iii) TRF analysis. Fresh BM cells from wild-type, DNA-PKcs$^{+/-}$, and DNA-PKcs$^{-/-}$ littermate mice, as well as from SCID mice and their corresponding wild types, were isolated as described above, and telomere restriction fragment (TRF) analysis was done as described by Blasco et al. (9).

G-strand overhang assay. The G-strand assay was performed as described previously (28) with minor modifications. Fresh BM cells and MEFs (10^6) from several pairs of wild-type mice and DNA-PKcs$^{-/-}$ littermates were included in restriction analysis grade agarose plugs in accordance with instructions provided by the manufacturer (Bio-Rad). After overnight digestion in LDS buffer (1% lithium dodecyl sulfate, 100 mM EDTA [pH 8.0], 10 mM Tris [pH 8.0]), the plugs were digested with either 0, 40, or 100 U of mung bean nuclease (MBN) for 15 min. Then the plugs were digested with *Mbo*I overnight and subjected to pulsed-field gel electrophoresis as described previously (9). The sequential in-gel hybridizations in native and denaturing conditions to visualize G-strand overhangs and telomeres, respectively, were carried out as described before (28). Quantification of the G-strand overhang radioactive signals was carried out using a STORM 860 PhosphorImager (Molecular Dynamics), using the software pro-

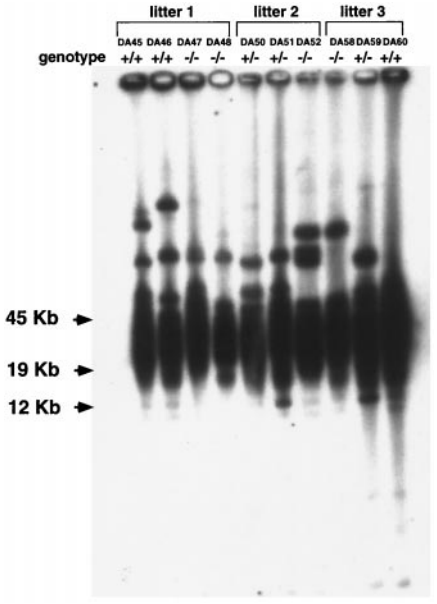

FIG. 3. TRF analysis of wild-type, DNA-PKcs$^{+/-}$, and DNA-PKcs$^{-/-}$ primary MEFs. Wild-type (+/+; DA45, DA46, and DA60), DNA-PKcs$^{+/-}$ (+/−; DA50, DA51, and DA59), and DNA-PKcs$^{-/-}$ (−/−; DA47, DA48, DA52, and DA58) littermate mice were studied. Notice that TRF signals are similar in DNA-PKcs$^{-/-}$, DNA-PKcs$^{+/-}$, and wild-type BM cells (see also Table 3 and Fig. 5 for other analyses of the same BM cells). Three litters were analyzed.

vided by the manufacturer. These values were corrected by the TRF signal in denaturing gel conditions.

Telomerase assay. S-100 extracts were prepared from wild-type, DNA-PKcs$^{+/-}$, and DNA-PKcs$^{-/-}$ primary MEF cultures, and a modified version of the TRAP assay was used to measure telomerase activity (8). An internal control for PCR efficiency was included (TRAPeze kit; Oncor).

RESULTS

DNA-PKcs is necessary to prevent telomere fusions and the formation of anaphase bridges during mitosis. Telomeres protect chromosome ends from degradation, end-to-end fusions, and recombination activities. To study the impact of DNA-PKcs deficiency on telomere function, we analyzed the involvement of telomeres in the chromosomal aberrations spontaneously arising in primary (passage 1) wild-type and DNA-PKcs$^{-/-}$ MEFs derived from heterozygous crosses. For this, we performed Q-FISH of metaphasic nuclei with a fluorescent telomeric peptide nucleic acid probe (47, 54) (see Materials and Methods for a description of different aberrations) and then scored spontaneously arising chromosome aberrations for 80 to 100 metaphases of each primary MEF culture. As displayed in Table 1, no statistically significant differences between the frequency of chromosome breaks and fragments detected in MEFs isolated from DNA-PKcs$^{-/-}$ cultures and that detected in wild-type controls were found (0.026 and 0.032 breaks plus fragments per metaphase, respectively; Student's *t* test, $P = 0.67475$). Similarly, no significant difference in the frequency of telomeric associations (chromosomes with four distinct telomere signals that are aligned less than one-half chromatid apart; Fig. 1A) between genotypes was found (0.015 and 0.012 telomeric associations per metaphase for DNA-PKcs$^{-/-}$ and wild-type MEFs, respectively) (Table 1). Interestingly, DNA-PKcs$^{-/-}$ MEFs showed an elevated frequency of telomeric fusions (two chromosomes which are fused by at least one telomere; Fig. 1A) compared to wild-type controls; the average frequencies of fusions per metaphase were 0.065 and 0.017 for DNA-PKcs$^{-/-}$ and wild-type MEFs, respectively (Fig. 1; Table 1). All Robersonian-like fusions found (chromosomes fused by their p arms) showed telomeres at the fusion point and were included in the group of telomeric fusions. It is worth noting that the difference in telomeric fusions between wild-type and DNA-PKcs$^{-/-}$ cells is highly significant (Student's *t* test, $P = 0.00037174$). The frequency of telomeric fusions found in the DNA-PKcs$^{-/-}$ primary MEFs was lower than that previously reported for SCID mouse cells (0.165 telomeric fusions per metaphase) which carry a leaky mutation in the DNA-PKcs gene (5). We cannot rule out the possibility that the higher chromosomal instability described for SCID cells is due to the higher passage number of the SCID MEFs used by Bailey et al. (5) compared with the passage 1 DNA-PKcs$^{-/-}$ MEFs used in this study.

Importantly, all chromosomal abnormalities present in DNA-PKcs$^{-/-}$ cells were also detected in primary Ku86$^{-/-}$ MEFs but at a significantly higher frequency (47), suggesting additional roles for the Ku86 protein at the telomeres independent of the activity of the DNA-PK complex.

It is important to note that Q-FISH analysis allowed us to determine that all telomeric fusions present in DNA-PKcs$^{-/-}$ cells contained intact telomeres at the fusion point with an average length of 64.4 ± 9.39 kb, suggesting that these fusions did not originate from a loss of telomeric sequences. A similar phenotype has been previously described for Ku86 deficiency (47).

Finally, loss of telomere function has been proposed to trigger breakage-fusion-bridge cycles (3, 16) through the formation of telomeric fusions and the occurrence of anaphase bridges during mitosis. Both types of chromosomal aberrations occur in tumors and are thought to be important for their clonal evolution and progression (20). In agreement with a role for DNA-PKcs in telomere function and chromosomal stability, we found that DNA-PKcs$^{-/-}$ MEFs showed a significantly

TABLE 4. Measurement by Flow-FISH of telomere length in splenocytes and BM cells obtained from SCID and wild-type mice

Mouse	Telomere length[a] for:	
	Splenocytes	BM cells
Scid 1	5.805	5.79
Scid 2	5.625	5.58
Scid 3	5.025	3.195
Scid 4	4.65	4.02
Scid 5	4.8	5.835
Wt 1	2.82	3.285
Wt 2	2.895	4.02
Wt 3	3.285	3.39
Wt 4	3.54	2.265
Wt 5	3.135	3.72

[a] Telomere length is expressed in arbitrary fluorescence units which have been normalized against a calibration curve on R and S cells (see Materials and Methods).

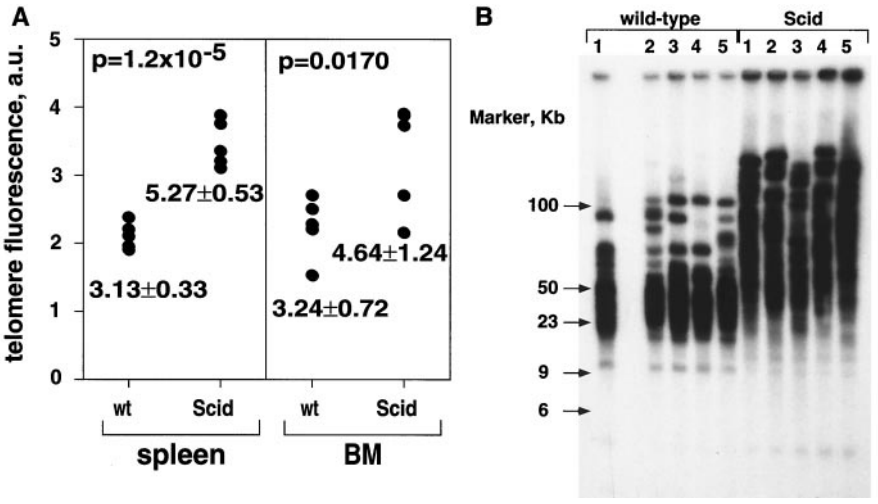

FIG. 4. Telomere length analysis of fresh BM cells and splenocytes from SCID and wild-type (wt) mice. (A) Flow-FISH. Telomere fluorescence (in arbitrary units [a.u.]) of splenocytes and BM cells as measured by flow cytometry for five different SCID and wt mice is shown. The average telomere lengths and standard deviations are indicated. The statistical significance of the difference in telomere fluorescence between SCID and wt mice is indicated by the Student's *t* test numbers (*P*). (B) TRF analysis. BM from wt and SCID mice in the same genetic background (see Materials and Methods) was used for TRF analysis. Notice that TRFs were dramatically elongated in SCID mice compared with wt controls.

higher frequency of anaphase bridges than control cells (0.16 and 0.70 anaphase bridges per anaphase scored for wild-type and DNA-PKcs$^{-/-}$ MEFs, respectively; 50 anaphases of each cell type were scored) (Fig. 1B shows examples). This difference is highly significant, as indicated by the Student *t* test value ($P = 0.0014$). Some anaphase bridges were still present at telophase in the DNA-PKcs$^{-/-}$ cells (Fig. 1B shows examples). Altogether, these results strongly suggest a role for DNA-PKcs in protecting chromosome ends and thus a role in genomic stability.

Normal length of TTAGGG repeats in DNA-PKcs-deficient cells. To determine if the protective role of DNA-PKcs at the telomere is mediated by the length of TTAGGG repeats, quantification of telomere length was carried out for littermate wild-type and DNA-PKcs$^{-/-}$ mice or embryos derived from heterozygous crosses. It is essential to compare littermate mice since mouse telomeres show individual variability (54). Q-FISH analysis of MEFs from wild-type and DNA-PKcs$^{-/-}$ littermate mice revealed that DNA-PKcs$^{-/-}$ cells had a telomere length similar to that of the wild type (Table 1). The average telomere lengths were 33.95 ± 0.2 and 35.0 ± 0.2 kb for MEFs from DNA-PKcs$^{-/-}$ (average of B6, C2, and C9) and wild-type (average of B5, C5, and C3) littermate mice, respectively (Fig. 2). The Q-FISH data on MEFs were confirmed by using a different technique to measure telomere fluorescence based on flow cytometry (Flow-FISH; described in Materials and Methods) (Table 2). In this case, average telomere fluorescence levels expressed in arbitrary units were 2.58 ± 0.1, 2.72 ± 0.2, and 2.71 ± 0.1 for DNA-PKcs$^{-/-}$ (average of A1, B4, B6, C2, and C9), DNA-PKcs$^{-/+}$ (average of A2 and B3), and wild-type (average of B5, C3, and C5) MEFs, respectively. Histograms showing the frequency of a given telomere fluorescence in MEFs from littermate wild-type (B5, C5, and C3) and DNA-PKcs$^{-/-}$ (B6, C2, and C9) mice are presented in Fig. 2. These histograms confirmed that the mean telomere fluorescence levels in DNA-PKcs$^{-/-}$ and wild-type MEFs are similar and furthermore showed that the levels of heterogeneity of telomeric lengths in both genotypes are similar (Fig. 2).

Flow-FISH studies on fresh splenocytes and BM cells derived from wild-type, DNA-PKcs$^{+/-}$, and DNA-PKcs$^{-/-}$ littermate mice (8 to 12 weeks old) also indicated that DNA-PKcs$^{-/-}$ telomeres were similar in length to those of wild-type littermates (Table 3), in agreement with the Q-FISH and Flow-FISH data for MEFs. These results were reproducible in at least six independent litters (Table 3).

Finally, telomere length was also evaluated by Southern blotting, as an alternative technique to measure telomere length not based on fluorescence. Primary BM cells from three wild-type, three DNA-PKcs$^{+/-}$, and four DNA-PKcs$^{-/-}$ mice were subjected to TRF analysis as described in Materials and Methods. As shown in Fig. 3, TRF analysis also showed similar telomere lengths in littermate mouse wild-type and DNA-PKcs$^{-/-}$ cells.

Altogether, these data demonstrate that a DNA-PKcs$^{-/-}$ deficiency in mammals does not result in significant telomere length alterations.

A spontaneous mouse mutation that also affects the DNA-PKcs locus but that produces a leaky phenotype is the mutation resulting in SCID mice (2, 11, 15, 33). Curiously, a previous report showed elongated telomeres in SCID mice compared to those in wild-type controls (26), which is in contrast to the normal-telomere-length phenotype displayed by DNA-PKcs$^{-/-}$ animals in this study. To rule out the possibility that possible technical differences between laboratories were the reason for this discrepancy, we measured telomere length for wild-type and SCID mice using the same methods used to measure telomere length in DNA-PKcs-deficient cells. First, we performed Flow-FISH of fresh splenocytes and BM cells isolated from five SCID and five wild-type mice in the same genetic background (see Materials and Methods). In agreement with results previously reported by Hande et al. (26), we

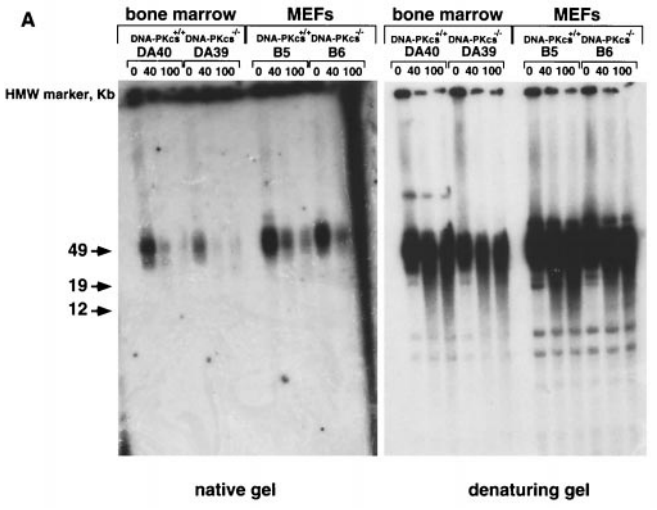

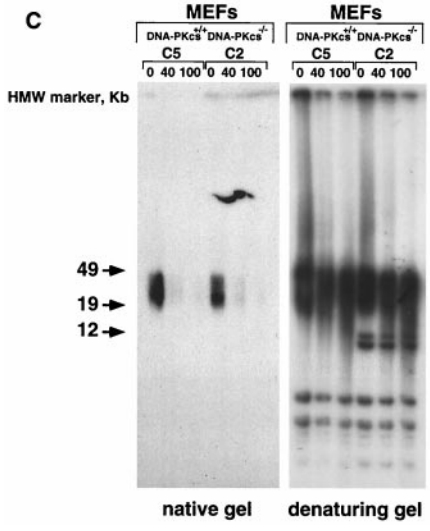

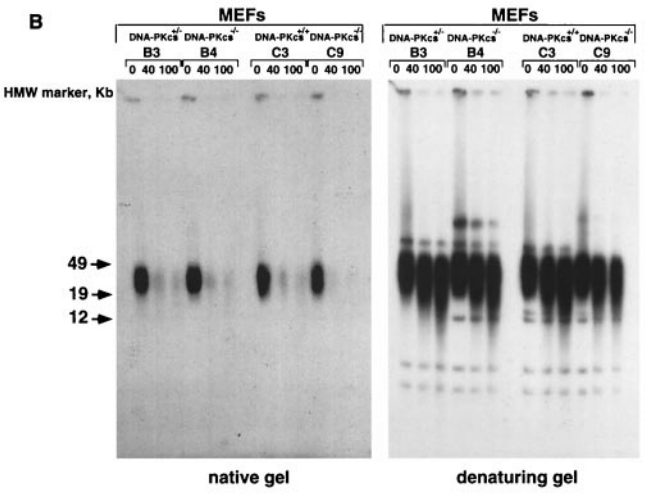

FIG. 5. Normal G-strand overhang in Ku86$^{-/-}$-deficient primary cells. G-strand overhangs in fresh BM cells or primary MEFs, as indicated, from littermate wild-type and DNA-PKcs$^{-/-}$ mice were visualized in native gel after hybridization with a $(CCCTAA)_4$ probe (see Materials and Methods). Notice that upon treatment with two different doses of MBN (40 and 100 U) the G-strand-specific signal decreases. As a control, the same gel was denatured and reprobed with the $(CCCTAA)_4$ probe to visualize telomeres. DA40 and DA39 are littermate wild-type and DNA-PKcs$^{-/-}$ mice, respectively. B3, B4, B5, and B6 are primary MEF cultures from littermates, as are C2, C3, C5, and C9. See Table 5 for quantification of G-strand-specific signals. HMW, high molecular weight.

found that SCID mouse telomeres were elongated compared with those of wild-type mice (Table 4; Fig. 4A). Average levels of telomere fluorescence for freshly isolated splenocytes from five different wild-type and SCID mice were 3.13 ± 0.33 and 5.27 ± 0.53, respectively. This difference was highly significant (Student's *t* test, $P = 1.2 \times 10^{-5}$). Similarly, average levels of telomere fluorescence for fresh BM cells from five different wild-type and SCID mice were 3.24 ± 0.72 and 4.64 ± 1.24, respectively. This difference was also significant (Student's *t* test, $P = 0.0170$). Furthermore, TRF analysis of five different wild-type and SCID mice also showed dramatically elongated telomeres in the SCID mice compared with the wild types (Fig. 4B). The elongated-telomere phenotype of SCID mice could also explain the difference in the frequency of telomeric fusions between SCID and DNA-PKcs$^{-/-}$ mice (see above). These results indicate fundamental differences between these two mouse models, at least in terms of telomere function. These differences can be explained if SCID mice carry other mutations besides the DNA-PKcs leaky mutation. Alternatively, the fact that SCID mice are not completely kinase null for the DNA-PKcs gene, and indeed express a different truncated form of the DNA-PKcs gene, could differentially affect telomere length and/or function.

Normal-length telomeric G-strand overhangs in DNA-PKcs$^{-/-}$ cells. G-strand overhangs are regions of G-rich single-stranded telomeric DNA that protrude in the 3′direction from the double-stranded telomere. These single-stranded G-rich regions have been recently involved in the formation of a special structure at the chromosome end named the T loop, which has been proposed to protect the ends from recombination and DNA repair activities (24). Hence, examination of

TABLE 5. Quantification of G-strand overhang signals

Mouse	Litter	Genotype	G-strand signal (%)[a]
DA40[b]	1	+/+	100.0
DA39[b]		−/−	49.5
B5[c]	2	+/+	100.0
B6[c]		−/−	88.1
B3[c]		+/−	100
B4[c]		−/−	109.2
C3[c]	3	+/+	100
C9[c]		−/−	86.5
C5[c]		+/+	100
C2[c]		−/−	75.9

[a] The percentage is expressed relative to the wild-type signal in each litter.
[b] Samples were obtained from the BM of adult mice.
[c] Samples were from MEFs.

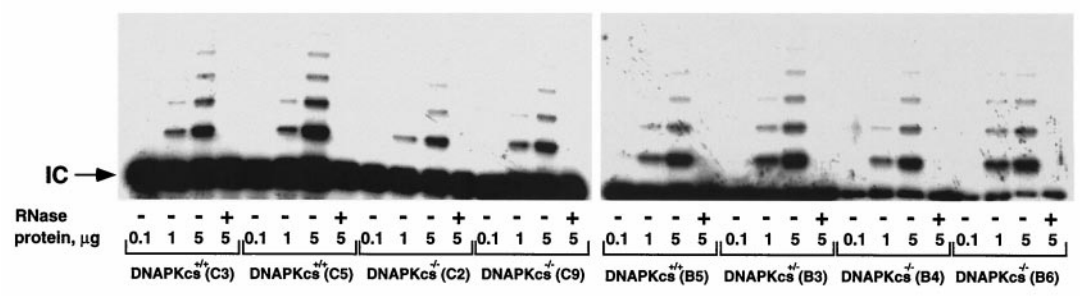

FIG. 6. Telomerase activity in wild-type and DNA-PKcs$^{-/-}$ MEFs. S-100 extracts were prepared from wild-type (C3, C5, and B5), DNA-PKcs$^{+/-}$ (B3), and DNA-PKcs$^{-/-}$ (C2, C9, B4, and B6) MEFs and assayed for telomerase activity. Extracts were pretreated (+) or not (−) with RNase. The protein concentrations used are indicated. Arrow, internal control (IC) for PCR efficiency. The same letter indicates littermate embryos.

telomeric G-strand overhangs in DNA-PKcs null cells was crucial to gain more insight into the abnormal frequency of telomeric fusions and anaphase bridges detected in these cells. To study the telomeric G-strand overhangs, we carried out TRF analysis with a $(CCCTAA)_4$ probe as described previously (28) using nondenaturing pulsed-field agarose gels (see Materials and Methods). Detection of a signal with the $(CCCTAA)_4$ probe hybridized to native DNA samples indicates the presence of the G-strand overhang. Freshly isolated BM cells, as well as primary MEFs from different littermate wild-type, DNA-PKcs$^{+/-}$, and DNA-PKcs$^{-/-}$ mice showed G-strand-specific signals that were similar in size and intensity in all genotypes (Fig. 5). Table 5 shows the quantification of the G-strand signals; the wild-type values were normalized to 100 in each litter. The average G-strand signal for DNA-PKcs$^{-/-}$ MEFs or BM cells was 81.8 ± 21.7% that for the wild types; this difference is not statistically significant (Student's t test, $P = 0.135$). To show that the probe specifically recognized the single-stranded telomeric tail, treatment with MBN, which specifically degrades single-stranded DNA and RNA overhangs, was performed. As expected, the G-strand signal decreased in all genotypes upon treatment, as shown in Fig. 5 ("native gel"). As a control, the same gel was denatured and rehybridized with the $(CCCTAA)_4$ probe, which highlighted the TRFs (Fig. 5; "denaturing gel"), again showing no difference in TRF lengths between wild-type, DNA-PKcs$^{+/-}$, and DNA-PKcs$^{-/-}$ phenotypes.

Collectively, these results show that DNA-PKcs deficiency in mammals does not result in the loss or shortening of the G-strand overhang at the telomeres. A similar result has been reported for the Ku86 deficiency, another member of the NHEJ pathway and component of the DNA-PK complex (47).

DNA-PKcs activity does not regulate telomerase activity. To investigate if the protein kinase activity of the DNA-PKcs subunit could have a regulatory role in telomerase activity (i.e., by phosphorylating the catalytic subunit of telomerase Tert), we quantified telomerase activity in three wild-type, one DNA-PKcs$^{+/-}$, and four DNA-PKcs$^{-/-}$ primary MEF cultures (passage 1) (see Materials and Methods). No significant difference in telomerase activity between wild-type and DNA-PKcs$^{-/-}$ littermates was detected (Fig. 6). This result indicates that lack of DNA-PK activity does not impact telomerase activity in mice and in turn is in agreement with the normal telomere length detected in DNA-PKcs-deficient cells.

DISCUSSION

The essential role of the DNA-PK complex in dsbr and V(D)J recombination in vertebrates is universally recognized. Biochemical analyses established that DNA-PK is a Ser/Thr kinase complex that must be bound to DNA in order to be activated. DNA-PK is composed of three subunits, a DNA end-binding component, which is a dimer of Ku70 and Ku86, and a large catalytic subunit of 460 kDa referred to as DNA-PKcs. Here we show that DNA-PKcs deficiency in mice results in increased end-to-end telomeric fusions and in a higher frequency of anaphase bridges in cells that otherwise show normal-length TTAGGG repeats at the telomeres and at the G-strand overhang. These results suggest a protective role for DNA-PKcs at the mammalian telomere that, in addition, is independent from the one conferred by telomeric repeats per se or by the length of the G-strand overhang. Telomeric fusions and anaphase bridges lead to breakage-fusion-bridge events, which in turn are important features found in human cancers (20).

An increase in the frequency of telomeric fusions has been recently reported for Ku86-deficient mice (47), suggesting that both Ku and DNA-PKcs have a role at the telomere. However, in contrast to DNA-PKcs-deficient cells, Ku86$^{-/-}$ cells show a slightly elongated telomere phenotype (47). These results suggest an additional role for the Ku86 protein at the telomere independent of that for the DNA-PK catalytic activity per se. This differential outcome between DNA-PKcs and Ku86 is not surprising if we consider that a mutation in Ku86 not only inactivates Ku86 per se but also impairs DNA-PK activity. This is also in agreement with the complex phenotype observed in Ku86$^{-/-}$ mice compared to DNA-PKcs$^{-/-}$ animals (18, 25, 43, 49, 51). Although Ku86 and DNA-PKcs gene products belong to the same enzymatic complex, several studies have demonstrated the differential role of these proteins in DNA repair and V(D)J recombination (18, 25, 43, 44, 49).

Our finding of increased telomeric fusions in DNA-PKcs null cells has been confirmed in recent experiments using SCID mice carrying a spontaneous rodent DNA-PKcs gene mutation (5). In contrast to what we found for DNA-PKcs

deficiency, however, Hande et al. (26) reported an elongated-telomere phenotype in the SCID mice compared to wild-type controls. Using Flow-FISH and TRF techniques, we have been able to confirm that SCID but not DNA-PKcs$^{-/-}$ mice show elongated telomeres compared with the corresponding wild-type controls. These results indicate fundamental differences between DNA-PKcs$^{-/-}$ and SCID mice, at least in terms of telomere function. These differences could be attributed (i) to the occurrence of still-to-be-defined additional mutations in the SCID strain which may affect telomere length, (ii) to the fact that SCID does not represent a null mutation for the DNA-PKcs gene and to potential residual kinase activity, and (iii) to the different types of truncation in the DNA-PKcs gene product in SCID and DNA-PKcs$^{-/-}$ cells that might impact the recruitment of other components necessary for telomere length regulation (2, 11, 15).

Collectively, these results indicate that the DNA-PK complex has a role in protecting telomeres from fusions. Interestingly, the DNA-PK complex is involved in dsbr in mammals by NHEJ; however, in combination with telomeric proteins, it might be involved in masking chromosome ends to prevent them from being recognized as DSBs. In fact, the telomere fusions detected in DNA-PKcs-deficient cells might represent NHEJ events. In this regard, mutations in DNA repair proteins do not abolish the capability of the cells to carry out NHEJ on broken ends (16, 36).

The end-to-end fusion phenotype has been previously recreated in cells that lack telomerase activity and that undergo progressive telomere shortening with increasing cell divisions (9). Likewise, cells expressing a dominant-negative mutation of the TRF2 gene had an end-to-end fusion phenotype with normal telomere length but with loss of G-strand overhang (24, 50). Since the protective functions of DNA-PKcs and Ku86 at the telomere are independent of the length of TTAGGG repeats and of the integrity of the telomeric G-strand overhang, this suggests that the DNA-PK complex acts at the telomere in a fundamentally different way than telomerase (8) or TRF2 (24, 50). However, it is still possible that DNA-PKcs and Ku act similarly to TRF2 but that their functions are more redundant, giving rise to a less severe phenotype.

There are a number of ways, not necessarily mutually exclusive, that DNA-PK might function in telomere protection. One is that the protein kinase activity of DNA-PKcs is employed to regulate the binding activities of other telomeric components. Alternatively, in light of the large size of DNA-PKcs, it is tempting to speculate that it might have a role as a scaffolding protein, recruiting several other factors to the telomere. These results warrant future studies involving the evaluation of a putative synergistic effect between DNA-PK components and telomere components as means to shed more light on the biology of telomeres.

ACKNOWLEDGMENTS

We thank R. Serrano and E. Santos for mouse care and genotyping, respectively.

E.S. and F.G. were supported by the Government of Madrid (CAM). G.E.T. is a scholar of the Leukemia and Lymphoma Society. The G.E.T. laboratory was supported by National Institutes of Health CA76409, American Cancer Society IN97T, and the Aids for Cancer Research Foundation. The M.A.B. laboratory was funded by the SWISS BRIDGE award, 2000, by the Ministry of Science and Technology (PM97-0133), Spain, by CAM 08.1/0030/98, by the European Union (EURATOM/991/0201, FIGH-CT-1999-00002, FIS5-1999-00055), and by the Department of Immunology and Oncology (DIO). The DIO is funded by the Spanish Council for Scientific Research and by Pharmacia Corporation.

F. A. Goytisolo and E. Samper contributed equally to this work.

REFERENCES

1. **Alexander, P., and Z. B. Mikulski.** 1961. Mouse lymphoma cells with different radiosensitivities. Nature **192:**572-573.
2. **Araki, R., A. Fujimori, K. Hamatani, K. Mita, T. Saito, M. Mori, R. Fukumura, M. Morimyo, M. Muto, M. Itoh, K. Tatsumi, and M. Abe.** 1997. Nonsense mutation at Tyr-4046 in the DNA-dependent protein kinase catalytic subunit of severe combined immune deficiency mice. Proc. Natl. Acad. Sci. USA **94:**2438–2443.
3. **Artandi, S. E., S. Chang, S.-L. Lee, S. Alson, G. J. Gottlieb, L. Chin, and R. DePinho.** 2000. Telomere dysfunction promotes nonreciprocal translocations and epithelial cancers in mice. Nature **406:**641–645.
4. **Autexier, C., and C. W. Greider.** 1996. Telomerase and cancer: revisiting the telomere hypothesis. Trends Biochem. **21:**387–391.
5. **Bailey, S. M., J. Meyne, D. J. Chen, A. Kurimasa, G. C. Li, B. E. Lehnert, and E. H. Goodwin.** 1999. DNA double-strand break repair proteins are required to cap the ends of mammalian chromosomes. Proc. Natl. Acad. Sci. USA **96:**14899–14904.
6. **Bianchi, A., and T. de Lange.** 1999. Ku binds telomeric DNA *in vitro*. J. Biol. Chem. **274:**21223–21227.
7. **Blackburn, E. H.** 1991. Structure and function of telomeres. Nature **350:** 569–573.
8. **Blasco, M. A., M. Rizen, C. W. Greider, and D. Hanahan.** 1996. Differential regulation of telomerase activity and telomerase RNA during multi-stage tumorigenesis. Nat. Genet. **12:**200–204.
9. **Blasco, M. A., H.-W. Lee, P. Hande, E. Samper, P. Lansdorp, R. DePinho, and C. W. Greider.** 1997. Telomere shortening and tumor formation by mouse cells lacking telomerase RNA. Cell **91:**25–34.
10. **Blasco, M. A., S. M. Gasser, and J. Lingner.** 1999. Telomeres and telomerase. Genes Dev. **13:**2353–2359.
11. **Blunt, T., D. Gell, M. Fox, G. E. Taccioli, A. R. Lehmann, S. P. Jackson, and P. A. Jeggo.** 1996. Identification of a non-sense mutation in the carboxyl terminal region of DNA-dependent protein kinase catalytic subunit in the SCID mouse. Proc. Natl. Acad. Sci. USA **93:**10285–10290.
12. **Boulton, S. J., and S. P. Jackson.** 1996. Identification of a *Saccharomyces cerevisiae* Ku80 homolog: roles in DNA double strand break rejoining and in telomeric maintenance. Nucleic Acids Res. **24:**4639–4648.
13. **Boulton, S. J., and S. P. Jackson.** 1998. Components of the Ku-dependent non-homologous end-joining pathway are involved in telomeric length maintenance and telomeric silencing. EMBO J. **17:**1819–1828.
14. **Counter, C. M., A. A. Avilion, C. E. LeFeuvre, N. G. Stewart, C. W. Greider, C. B. Harley, and S. Bacchetti.** 1992. Telomere shortening associated with chromosome instability is arrested in immortal cells which express telomerase activity. EMBO J. **11:**1921–1929.
15. **Danska, J. S., D. P. Holland, S. Mariathasa, K. M. Williams, and C. J. Guidos.** 1996. Biochemical and genetic defects in the DNA-dependent protein kinase in murine scid lymphocytes. Mol. Cell. Biol. **16:**5507–5517.
16. **de Lange, T.** 1995. Telomeres, p. 265–293. Cold Spring Harbor Press, Cold Spring Harbor, N.Y.
17. **DiBiase, S. J., Z. C. Zeng, R. Chen, T. Hyslop, W. J. Curran, Jr., and G. Iliakis.** 2000. DNA-dependent protein kinase stimulates an independently active, nonhomologous, end-joining apparatus. Cancer Res. **60:**1245–1253.
18. **Gao, Y., J. Chaudhuri, C. Zhu, L. Davidson, D. T. Weaver, and F. W. Alt.** 1998. A targeted DNA-PKcs-null mutation reveals DNA-PK-independent functions for Ku in V(D)J recombination. Immunity **9:**367–376.
19. **Gao, Y., D. O. Ferguson, W. Xie, J. P. Manis, J. Sekiguchi, K. M. Frank, J. Chaudhuri, J. Horner, R. A. DePinho, and F. W. Alt.** 2000. Interplay of p53 and DNA-repair protein XRCC4 in tumorigenesis, genomic stability and development. Nature **404:**897–900.
20. **Gisselsson, D., L. Pettersson, M. Hoglund, M. Heidenblad, L. Gorunova, J. Wiegant, F. Mertens, P. Dal Cin, F. Mitelman, and N. Mandahl.** 2000. Chromosomal breakage-fusion-bridge events cause genetic intratumor heterogeneity. Proc. Natl. Acad. Sci. USA **97:**5357–5362.
21. **Gravel, S., M. Larrivee, P. Labrecque, and R. J. Wellinger.** 1998. Yeast Ku as a regulator of chromosomal DNA end structure. Science **280:**741–744.
22. **Grawunder, U., M. Wilm, X. Wu, P. Kulesza, T. E. Wilson, M. Mann, and M. Lieber.** 1997. Activity of DNA ligase IV stimulated by complex formation with XRCC4 protein in mammals. Nature **388:**492–495.
23. **Greenwall, P. W., S. L. Kronmal, S. E. Porter, J. Gassenhuber, B. Obermaier, and T. D. Petes.** 1995. Tel1, a gene involved in controlling telomere length in S. cerevisiae, is homologous to the human ataxia telangiectasia gene. Cell **82:**823–829.
24. **Griffith, J. D., L. Comeau, S. Rosenfield, R. M. Stansel, A. Bianchi, H. Moss, and T. de Lange.** 1999. Mammalian telomeres end in a large duplex loop. Cell **97:**503–514.

25. **Gu, Y. S., S. F. Jin, Y. J. Gao, D. T. Weaver, and F. W. Alt.** 1997. Ku70 deficient embryonic stem cells have increased ionizing radiosensitivity, defective DNA end binding activity, and inability to support V(D)J recombination. Proc. Natl. Acad. Sci. USA **94:**8076–8081.
26. **Hande, P., P. Slijepcevic, A. Silver, S. Bouffler, P. van Buul, P. Bryant, and P. Lansdorp.** 1999. Elongated telomeres in scid mice. Genomics **56:**221–223.
27. **Hartley, K. O., D. Gell, G. C. M. Smith, H. Zhang, N. Divecha, M. A. Conolley, A. Admon, S. P. Lees-Miller, C. W. Anderson, and S. P. Jackson.** 1995. DNA-dependent protein kinase catalytic subunit: a relative of phosphatidylinositol 3-kinase and the ataxia telangiectasia gene product. Cell **82:**849–856.
28. **Hemann, M. T., and C. W. Greider.** 1999. G-strand overhangs on telomeres in telomerase deficient mouse cells. Nucleic Acids Res. **27:**3964–3969.
29. **Herrera, E., E. Samper, J. Martín-Caballero, J. M. Flores, H.-W. Lee, and M. A. Blasco.** 1999. Disease states associated to telomerase deficiency appear earlier in mice with short telomeres. EMBO J. **18:**2950–2960.
30. **Herrera, E., C. Martinez, and M. A. Blasco.** 2000. Impaired germinal center formation in telomerase-deficient mice. EMBO J. **19:**472–481.
31. **Hsu, H.-L., D. Gilley, E. Backburn, and D. J. Chen.** 1999. Ku is associated with the telomere in mammals. Proc. Natl. Acad. Sci. USA **96:**12454–12458.
32. **Hsu, H.-L., D. Gilley, S. A. Galande, M. P. Hande, B. Allen, S.-H. Kim, G. C. Li, J. Campisi, T. Kowhi-Shigematsu, and D. J. Chen.** 2000. Ku acts in a unique way at the mammalian telomere to prevent end joining. Genes Dev. **14:**2807–2812.
33. **Kirchgessner, C. U., C. K. Patil, J. W. Evans, C. A. Cuomo, L. M. Fried, T. Carter, M. A. Oettinger, and J. M. Brown.** 1995. DNA-dependent kinase (p350) as a candidate gene for the murine SCID defect. Science **267:**1178–1183.
34. **Lansdorp, P. M., N. P. Verwoerd, F. M. van de Rijke, V. Dragowska, M.-T. Little, R. W. Dirks, A. K. Raap, and H. J. Tanke.**1996. Heterogeneity in telomere length of human chromosomes. Hum. Mol. Genet. **5:**685–691.
35. **Laroche, T., S. G. Martin, M. Gotta, H. C. Gorham, F. E. Pryde, E. J. Louis, and S. M. Gasser.** 1998. Mutation of yeast Ku genes disrupts the subnuclear organization of telomeres. Curr. Biol. **8:**653–656.
36. **Li, G. C., H. H. Ouyang, X. L. Li, H. Nagasawa, J. B. Little, D. J. Chen, C. C. Ling, Z. Fuks, and C. Cordón-Cardó.** 1998. ku70: a candidate tumor suppressor gene for murine T cell lymphoma. Mol. Cell **2:**1–8.
37. **Li, Z., T. Otevrel, Y. Gao, H.-L. Cheng, B. Seed, T. D. Stamato, G. E. Taccioli, and F. W. Alt.** 1995. The XRCC4 gene encodes a novel protein involved in DNA double-strand break repair and V(D)J recombination. Cell **83:**1079–1089.
38. **Martin, S. G., T. Laroche, N. Suka, M. Grunstein, and S. M. Gasser.** 1999. Relocalization of telomeric Ku and SIR proteins in response to DNA double-strand breaks. Cell **97:**621–633.
39. **Metcalfe, J. A., J. Parkhill, L. Campbell, M. Stacey, P. Biggs, P. J. Byrd, and A. M. Taylor.** 1996. Accelerated telomere shortening in ataxia telangiectasia. Nat. Genet. **13:**350–353.
40. **Mills, K. D., D. A. Sinclair, and L. Guarente.** 1999. MEC1-dependent redistribution of the Sir3 silencing protein from telomeres to DNA double-strand breaks. Cell **97:**609–620.
41. **Morrow, D. M., D. A. Tagle, Y. Shiloh, F. S. Collins, and P. Hieter.** 1995. Tel 1, an S. cerevisiae homolog of the human gene mutatedin ataxia telangiectasia, is functionally related to the yeast checkpoint gene MEC1. Cell **82:**831–840.
42. **Nugent, C. I., G. Bosco, L. O. Ross, S. K. Evans, A. P. Salinger, J. K. Moore, J. E. Haber, and V. Lundblad.** 1998. Telomere maintenance is dependent on activities required for end repair of double-strand breaks. Curr. Biol. **8:**657–660.
43. **Nussenzweig, A., C. H. Chen, V. D. Soares, M. Sanchez, M. C. Sokol, M. C. Nussenzweig, and G. C. Li.** 1996. Requirement for Ku80 in growth and immunoglobulin V(D)J recombination. Nature **382:**551–555.
44. **Ouyang, H., A. Nussenzweig, A. Kurimasa, V. D. Soares, X. L. Li, C. Cordón-Cardó, W. H. Li, N. Cheong, M. Nussenzweig, G. Iliakis, D. J. Chen, and G. C. Li.** 1997. Ku70 is required for DNA repair but not for T cell antigen receptor gene recombination *in vivo*. J. Exp. Med. **186:**921–929.
45. **Poltoratsky, V. P., X. Shi, J. D. York, M. R. Lieber, and T. H. Carter.** 1995. Human DNA-activated protein kinase (DNA-PK) is homologous to phosphatidylinositol kinases. J. Immunol. **155:**4529–4533.
46. **Rufer, N., W. Dragowska, G. Thornbury, E. Roosnek, and P. M. Lansdorp.** 1998. Telomere length dynamics in human lymphocyte subpopulations measured by flow cytometry. Nat. Biotechnol. **16:**743–747.
47. **Samper, E., F. Goytisolo, P. Slijepcevic, P. van Buul, and M. A. Blasco.** 2000. Mammalian Ku86 prevents telomeric fusions independently of the length of TTAGGG repeats and the G-strand overhang. EMBO Rep. **1:**244–252.
48. **Smith, G. C. M., and S. P. Jackson.** 1999. The DNA-dependent protein kinase. Genes Dev. **13:**916–934.
49. **Taccioli, G. E., A. G. Amatucci, H. J. Beamish, D. Gell, X. H. Xiang, M. I. Torres Arzayus, A. Priestley, S. P. Jackson, A. Marshak Rothstein, P. A. Jeggo, and V. L. Herrera.** 1998. Targeted disruption of the catalytic subunit of the DNA-PK gene in mice confers severe combined immunodeficiency and radiosensitivity. Immunity **3:**355–366.
50. **van Steensel, B., A. Smogorzewska, and T. de Lange.** 1998. TRF2 protects human telomeres from end-to-end fusions. Cell **92:**401–413.
51. **Vogel, H., D.-S. Lim, G. Karsenty, M. Finegold, and P. Hasty.** 1999. Deletion of Ku86 causes early onset of senescence in mice. Proc. Natl. Acad. Sci. USA **96:**10770–10775.
52. **Zhu, C. M., M. A. Bogue, D. S. Lim, P. Hasty, and D. B. Roth.** 1996. Ku86-deficient mice exhibit severe combined immunodeficiency and defective processing of V(D)J recombination intermediates. Cell **86:**379–389.
53. **Zhu, X. D., B. Kuster, M. Mann, J. H. Petrini, and T. de Lange.** 2000. Cell-cycle-regulated association of RAD50/MRE11/NBS1 with TRF2 and human telomeres. Nat. Genet. **25:**347–352.
54. **Zijlmans, J. M., U. M. Martens, S. Poon, A. K. Raap, H. J. Tanke, R. K. Ward, and P. M. Lansdorp.** 1997. Telomeres in the mouse have large inter-chromosomal variations in the number of T_2AG_3 repeats. Proc. Natl. Acad. Sci. USA **94:**7423–7428.